Georg-August-Universität Göttingen

Investigation of resolution requrements for wall-modelled LES of attached and massively separated flows at high Reynolds numbers

Zhang, X., Knopp, T., Valentino, M., Kessler, R., Lube, G.

Nr. 2008-18

Preprint-Serie des
Instituts für Numerische und Angewandte Mathematik
Lotzestr. 16-18
D - 37083 Göttingen

Investigation of resolution requirements for wall-modelled LES of attached and massively separated flows at high Reynolds numbers

Xiaoqin Zhang[1], Tobias Knopp[2], Mariafrancesca Valentino[2], Roland Kessler[2], and Gert Lube[3]

[1] School of Mechanical and Aerospace Engineering, Nanyang Technological University, 50, Nanyang Avenue, 639798, Singapore, xqzhang@ntu.edu.sg,
[2] DLR Göttingen, AS-C^{2}A^{2}S^{2}E, Bunsenstr. 10, D-37073 Göttingen, Germany,
[3] Institut für Numerische und Angewandte Mathematik, Georg-August-Universität Göttingen, Lotzestrasse 16-18, D-37083 Göttingen, Germany

Summary

This work is dedicated to the resolution requirements of Large-Eddy Simulation (LES) with near-wall modelling for attached and massively separated flows at high Reynolds numbers using the DLR THETA code. Two sensors are proposed to measure the resolution quality of LES for statistically steady flows. The first sensor is based on the resolved turbulent kinetic energy and the second one considers the resolved turbulent shear stress. These sensors are applied to turbulent channel flow at $Re_\tau = 4800$ and to the flow over a backward-facing step at $Re_h = 37500$ on successively refined meshes, and results are compared with a convergence study of the mean velocity profiles.

1 Introduction

One of the major problems in large-eddy simulation of turbulent flows concerns assessing reliability of the LES results in terms of numerical resolution. Even for fully developed turbulent channel flow, results become poor if the mesh (or the time step) is not fine enough, in particular if using methods that rely on low-order schemes. This issue cannot be overestimated also from an industrial point of view. For industrial applications of LES to flows in complex geometries, grid convergence cannot be reached or ensured by a global mesh refinement study due to extremely large computational costs.

In the present work we focus on the spatial discretisation error for statistically steady flows. As a solution strategy for *statistically steady* flows, this work presents two sensors to measure the resolution quality of the LES in order to ensure that turbulent flow features are properly resolved. These sensors may then be used as a refinement indicator for local mesh adaptation. The final aim is to ensure high quality LES results by providing a tool for automatic grid refinement for LES and thereby reducing the large expertize on proper use of LES demanded from the CFD code user.

The concept of sensor-based mesh adaptation for LES was proposed by [10] with focus on a so-called *adaptive LES*, where $\Delta = \Delta(x)$ is interpreted as a model parameter, and, if the ratio h/Δ is fixed, Δ is adapted by varying the mesh spacing until a desired turbulence resolution is obtained. In [10], only an abstract formula for turbulence resolution defined by the fraction of resolved to total turbulent kinetic energy is given. An operational formula was proposed in [7] and tested for free-shear layers and regions of separated flow. In the present work, this approach is extended to attached boundary layer flows by investigating a sensor based on the ratio of resolved to total turbulent shear stress. Alternative approaches attempt to separate the influence of the numerical error and the contribution of the subgrid-scale model, see [2], [6].

2 Basic discretization and turbulence modelling

The DLR THETA code is the unstructured solver for flows with small compressibility effects developed at DLR Göttingen based on a finite volume scheme on collocated grids. It uses a projection method to split the calculation of velocity $\boldsymbol{u}$ and pressure p governed by the Navier-Stokes equations

$$\begin{aligned} \partial_t \boldsymbol{u} - \boldsymbol{\nabla} \cdot (2\nu \mathbb{S}(\boldsymbol{u})) + \boldsymbol{\nabla} \cdot (\boldsymbol{u} \otimes \boldsymbol{u}) + \boldsymbol{\nabla} p = \boldsymbol{f} \quad & \text{in } \Omega \times (0,T] \\ \boldsymbol{\nabla} \cdot \boldsymbol{u} = 0 \quad & \text{in } \Omega \times (0,T] \end{aligned}$$

with the rate of strain tensor $\mathbb{S}(\boldsymbol{u}) = \frac{1}{2}(\boldsymbol{\nabla}\boldsymbol{u} + \boldsymbol{\nabla}\boldsymbol{u}^T)$, viscosity ν and source term $\boldsymbol{f}$. The interpolation scheme by Rhie and Chow [11] is applied to avoid spurious pressure oscillations.
The enhancement of the THETA code for LES-type simulations was demonstrated in [12]. Key elements of a proper numerical method are using central difference scheme (CDS) for the convective fluxes in divergence form and a second order time discretisation using the second order backward differencing formula BDF(2). Diffusive fluxes are discretized with the CDS. The classical Smagorinsky model is employed as subgrid scale (SGS) model together with van Driest damping for wall-bounded flows

$$\nu_{\mathrm{t}} = (C_S \mathcal{D}(y^+)\Delta)^2 |\mathbb{S}| \,, \qquad \mathcal{D}(y^+) = 1 - \exp(-y^+/A^+) \,, \quad A^+ = 26$$

with $|\mathbb{S}| = (2\mathbb{S}(\boldsymbol{u}) : \mathbb{S}(\boldsymbol{u}))^{1/2}$ where $\mathbb{A} : \mathbb{B} = \sum_{i,j=1}^{d} A_{ij} B_{ij}$, friction velocity u_τ, and wall-distance in viscous units $y^+ = y u_\tau / \nu$ with viscosity ν.
Alternatively, we use the wall-adapting local eddy-viscosity (WALE) model [9]

$$\nu_t = C_w \Delta^2 \frac{(S^d_{ij} S^d_{ij})^{3/2}}{(S_{ij} S_{ij})^{5/2} + (S^d_{ij} S^d_{ij})^{5/4}}$$

with $S_{ij} = (\mathbb{S}(\boldsymbol{u}))_{ij}$ and S^d_{ij} defined by

$$S^d_{ij} = \frac{1}{2}\left(g^2_{ij} + g^2_{ji}\right) - \frac{1}{3}\delta_{ij} g^2_{kk} \,, \quad g^2_{ij} = g_{ik} g_{kj} \,, \quad g_{ij} = \frac{\partial u_i}{\partial x_j}$$

where the constant is $C_w = 0.1$ for boundary layer flows.
Results for the low Reynolds number benchmark test cases decaying isotropic turbulence (DIT) and turbulent channel flow at $Re_\tau = 395$ are in very good agreement with results found in literature, see Fig. 1- 2. Interestingly, for channel flow at $Re_\tau = 395$, even on the 64x64x64 mesh, the resolution is not fine enough.
In order to assess the spatial resolution quality of a large-eddy simulation, the aim is to design a sensor S which takes a value in $[0, 1]$ for each control volume of the finite-volume mesh. Moreover we have to specify threshold values s_0, s_1. Then $S > s_1$ indicates that the local mesh resolution is sufficiently fine and $S < s_0$ if the mesh is too coarse.
Recently, an indicator based on the resolved turbulent kinetic energy to measure the resolution quality of statistically steady free-shear layers has been proposed, cf. [7],

$$S_k(\boldsymbol{x}) \;=\; \frac{k}{k + k_{\mathrm{sgs}}}\,, \quad k = \frac{1}{2}\langle(\boldsymbol{u} - \langle\boldsymbol{u}\rangle)^2\rangle\,, \quad k_{\mathrm{sgs}} = \frac{1}{2}\langle(\boldsymbol{u} - \overline{\boldsymbol{u}})^2\rangle \qquad (1)$$

where $\langle\cdot\rangle$ denotes the filtering operator in homogeneous directions and in time and the spatial average $\overline{\boldsymbol{u}}$ is defined by the convolution integral

$$\overline{\boldsymbol{u}}(x,t) \;=\; \int_{\mathbb{R}^d} g_\Delta(\boldsymbol{x} - \boldsymbol{y})\boldsymbol{u}(\boldsymbol{y},t)\mathrm{d}\boldsymbol{y}$$

with g_Δ being the top hat filter function. The turbulent kinetic energy in the residual or subgrid scale motion cannot be computed from resolved quantities and hence requires modelling. The idea of (1) is to use a scale similarity assumption for the subgrid scale velocity $\boldsymbol{u}_{\mathrm{sgs}} \approx \boldsymbol{u}(\boldsymbol{x},t) - \overline{\boldsymbol{u}}(\boldsymbol{x},t)$.
An alternative indicator considers the ratio of resolved to total shear stress and may be defined by

$$S_s(\boldsymbol{x}) \;=\; \frac{\tau}{\tau + \tau_{\mathrm{sgs}}}\,, \quad \tau = \langle u'v'\rangle\,, \quad \tau_{\mathrm{sgs}} = -\langle\nu_t\rangle\langle\frac{du}{dy}\rangle. \qquad (2)$$

For channel flow at $Re_\tau = 395$, these two grid quality indicators (1) and (2) are shown in Fig. 3. Values of indicator (1) are close to 1.0 even on the coarsest mesh. Therefore an improved resolution with decreasing grid spacing can hardly be judged from this sensor for wall-bounded flow. On the other hand, indicator (2) shows a clear trend of improved resolution with decreasing grid spacing. On the 96x96x96 mesh, the indicator for resolved stresses takes values of 0.9 except in the viscous sublayer. This seems to be the minimal required value for wall-resolved LES.

3 Presentation of results for high Reynolds number flows

For flows at higher Reynolds number, wall functions are used to bridge the near-wall region. The wall node is shifted to a user specified position y_δ into the cell adjacent to the wall. Denote $y(1)$ the wall distance of the first node above the wall. Then we use $y_\delta = 0.27y(1)$, which ensures that both y_δ and $y(1)$ are close to the center of

their respective control volumes. The universal velocity profile of RANS-type by Reichardt is matched with the instantaneous LES solution at the shifted node y_δ for computing the wall-shear stress, see [7].

3.1 Turbulent channel flow at $Re_\tau = 4800$

We consider turbulent channel flow at $Re_\tau = 4800$. Numerical results are compared also with the data by Comte-Bellot [1]. However, for the three cases considered by Comte-Bellot ($Re_\tau = 2340$, 4800, 8160) the values obtained for slope $1/\kappa$ and constant C of the log law $u^+ = \log(y^+)/\kappa + C$ show a significant spreading and also deviate from the standard values.
The role of the time discretisation error for this flow was studied in [7], showing that $\delta t^+ \equiv \delta t u_\tau^2/\nu = 1.75$ is required to ensure that time discretisation error is sufficiently small. Regarding the spatial discretisation error three meshes are considered with varying mesh size in streamwise and spanwise direction. Meshes of $N_x \times 24 \times N_z$ nodes with $N_x = N_z \in \{64, 96, 128\}$ correspond to $\Delta x^+ = 2\Delta z^+ = 470, 317, 235$. For all meshes $y_\delta^+ = 50$ for the shifted node. The profiles for mean velocity and for the sensor based on resolved stress (2) are plotted in Fig. 4. The log-layer mismatch on the $N_x = 64$-mesh appears in conjunction with a too low resolution of the turbulent shear stress. A resolution of 90% of the turbulent shear stress appears to be necessary to remove the log-layer mismatch, which can be achieved only on the finest mesh. Note that the corresponding spacing $\Delta x^+, \Delta z^+$ is already little coarse compared to existing best practice guidelines for LES with near-wall modelling using wall functions.

3.2 Flow over a backward-facing step at $Re_h = 37500$

Then we consider the turbulent flow over a backward-facing step at Reynolds number $Re_h = U_0 h/\nu = 37500$ based on step height h, studied experimentally by Driver and Seegmiller [4]. Regarding the computational domain used, the length of the inflow part is $4h$ before the step with channel height $8h$ and the channel length after the step is $25h$. At the inlet, the mean velocity profile is prescribed by blending of DNS data in the near-wall region and experimental data [4] in the outer part. The method by [5] is used to generate turbulent structures at the inflow boundary.
The mesh spacing is almost equidistant in $x-$ and $z-$direction and only a small stretching is applied in $x-$direction near the outlet. Wall functions are used on top and bottom wall. The role of the time step size was studied in [7] showing that for $\delta t = 1 \times 10^{-5}[s]$ the time-discretisation error is sufficiently small. After a flow developing time of $348h/U_0$, which is around 12 "flow through" times, the average is computed over a sample time $348h/U_0$, and in spanwise direction.
The aim of a sensor is to assess the mesh resolution without need to perform a global refinement study. Profiles for mean velocity at 8 cross sections and the corresponding experimental data are shown in Fig. 5. The resolution is satisfactory on the finest mesh (219x89x32 nodes), but not on the medium mesh (110x47x32 nodes). Fluctuations, omitted here due to lack of space, are shown in [7]. In order to *develop* such

a sensor, we proceed in opposite direction. The first step is to perform a convergence study, and to consider the corresponding distribution of the sensor values. The distributions for the sensors in (1), (2) averaged over time and in spanwise direction, on the medium mesh and on the finest mesh are shown in Fig. 6, 7.
An appropriate sensor has to satisfy the following property: Its values should increase monotonically when refining the mesh. This property may be observed only for special flow regions, e.g., attached boundary layer flows or free-shear layers. Indeed, the two sensors (1) and (2) appear to be suitable for different flow regions.
The sensor values for resolved turbulent kinetic energy (1) increase clearly in the region of the free shear layer and in the recirculation region when refining the mesh. The sensor values also increase inside the boundary layers, but not so obvious as in the other two regions, see also the results for channel flow at $Re_\tau = 395$.
On the other hand, the sensor values for resolved turbulent shear stress (2) are monotonically increasing in the attached boundary layer flow before the step with increasing spatial resolution, confirming results for turbulent channel flow at $Re_\tau = 4800$, see Fig. 4. But the sensor values do not show monotonically increasing behaviour in the free-shear layer and in the entire recirculation region.
The next step is to specify threshold values s_0, s_1. $S > s_1$ indicates that mesh resolution is sufficiently fine and $S < s_0$ if the mesh is too coarse. For the indicator (1) we suggest $s_0 = 0.8$ and $s_1 = 0.9$, see also [7]. Regarding indicator (2), it takes values around 0.875 in the largest part of the boundary layer before the step on the finest mesh. Little uncertainty in the results may stem from using synthetic turbulence at the inlet. Together with the results for channel flow at $Re_\tau = 4800$, we suggest $s_0 = 0.8$ and $s_1 = 0.9$ which might be little conservative.

4 Conclusion

The resolution requirements of LES for attached and massively separated flows have been considered. For statistically steady flows, two sensors to measure the resolution quality of LES have been presented and compared. A first sensor based on the resolved turbulent kinetic energy appears suitable for free shear layers and regions of separated flow. A second sensor based on the resolved shear stress seems suitable for regions of attached boundary layer flow. The predictions of the sensors are supported by a mesh convergence study and with existing best-practice guidelines for attached equilibrium boundary layer flows.

Acknowledgements

The authors are grateful to Dr. Markus Klein for providing the routines for generating synthetical turbulence at inlet boundaries and helpful assistance in using them.

References

[1] AGARD: ”A selection of test cases for the validation of large-eddy simulations of turbulent flows”. Tech. rep., AGARD-AR-345, 1998.

[2] Celik, I., Cehreli, Z. and Yavuz, I.: "Index of resolution quality for large eddy simulations". ASME Journal of Fluids Engineering **126**, 949–958, 2005.
[3] Comte-Bellot, G., Corrsin, S.: "Simple Eulerian time correlation of full- and narrow-band velocity signals in grid-generated, 'isotropic' turbulence". Journal of Fluid Mechanics **48(2)**, 273–337, 1971.
[4] Driver, D. M., Seegmiller, H. L.: "Features of a reattaching turbulent shear layer in divergent channel flow". AIAA Journal **23**, 163-171, 1985.
[5] Klein, M., Sadiki, A., Janicka, J.: "A digital filter based generation of inflow data for spatially developing direct numerical or large eddy simulations". Journal of Computational Physics **186**, 1652–1665, 2003.
[6] Klein, M.: "An attempt to assess the quality of large eddy simulations in the context of implicit filtering". Flow, Turbulence and Combustion **75**, 131–147, 2005.
[7] Knopp, T., Zhang, X. Q., Kessler, R., Lube, G.: "Enhancement of an Industrial Finite-Volume Code for Large-Eddy-Type Simulation of Incompressible High-Reynolds Number Flow Using Near-Wall Modelling". *submitted to* Computer Methods in Applied Mechanics and Engineering, 2008.
[8] Moser, R.D., Kim, J., Mansour, N.N.: "Direct numerical simulation of turbulent channel flow up to $Re_\tau = 590$". Physics of Fluids **11**, 943–946, 1999.
[9] Nicoud, F., Ducros, F.: "Subgrid-scale stress modelling based on the square of the velocity gradient tensor". Flow, Turbulence and Combustion **62**, 183-200, 1999.
[10] Pope, S.B.: "Ten questions concerning the large-eddy simulation of turbulent flows". New Journal of Physics **6**, 1–24, 2004.
[11] Rhie, C. M., Chow, W. L.: "Numerical study of the turbulent flow past an airfoil with trailing edge separation". AIAA Journal **21**, 1525–1532, 1983.
[12] Zhang, X. Q.: "Identification of model and grid parameters for incompressible turbulent flows". Ph. D. thesis, University Göttingen, 2007.

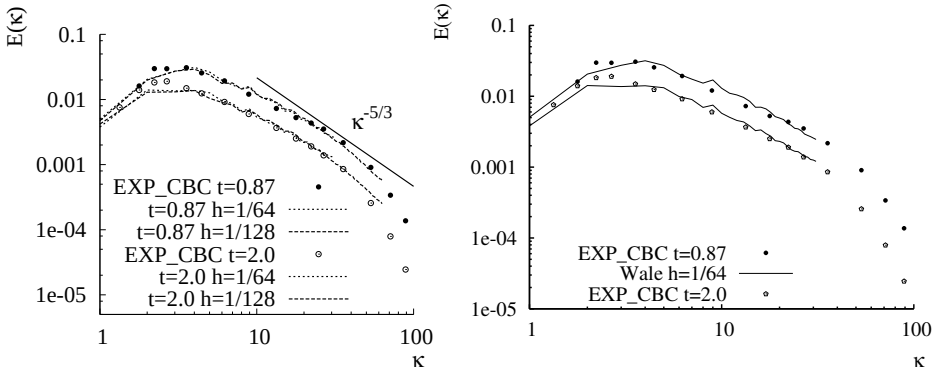

Figure 1 DIT testcase by Comte-Bellot [3]: Energy spectrum. Standard Smagorinsky model for $N = 64$ with $C_S = 0.1$ and for $N = 128$ with $C_S = 0.094$ (left). WALE model for $N = 64$ with $C_w = 0.55$ (right).

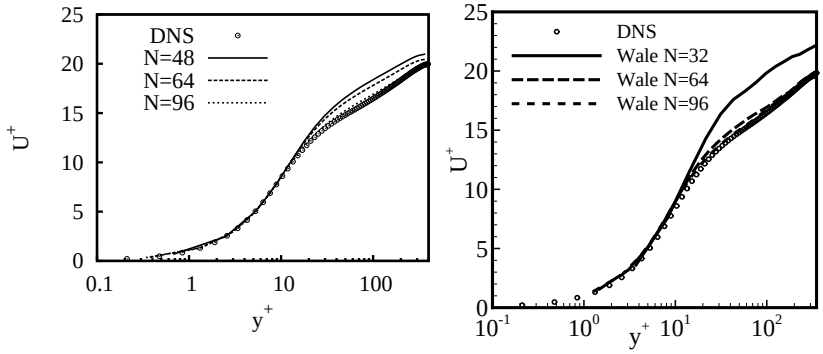

Figure 2 Channel flow at $Re_\tau = 395$ by [8]: Mean velocity profile for different spatial resolutions. Standard Smagorinsky with $C_S = 0.1$ (left). WALE with $C_w = 0.1$ (right).

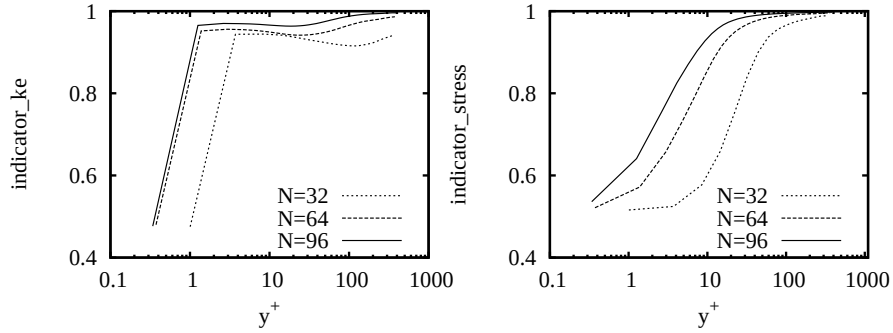

Figure 3 Channel flow at $Re_\tau = 395$ by [8]: Profile for sensor for LES resolution quality based on resolved turbulent kinetic energy (1) (left) and based on resolved stress (2) (right).

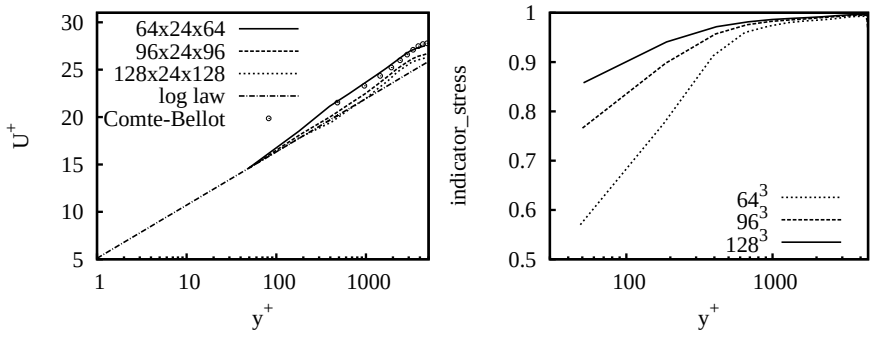

Figure 4 Turbulent channel flow at $Re_\tau = 4800$. Left: Mean velocity profiles for different spatial resolutions. Right: Sensor based on resolved shear stress (2).

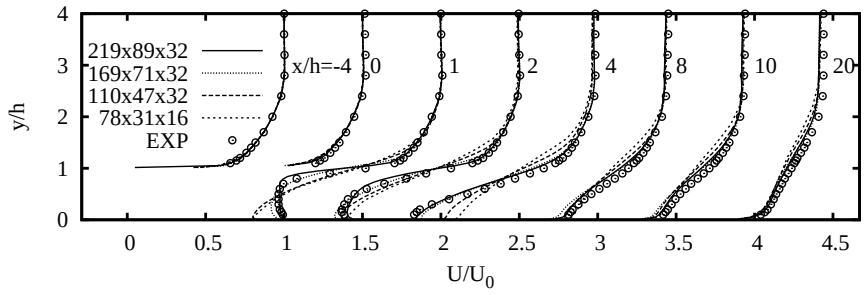

Figure 5 Flow over backward facing step at $Re_h = 37500$ by [4]: Convergence study of mean velocity profiles at several streamwise positions using different meshes.

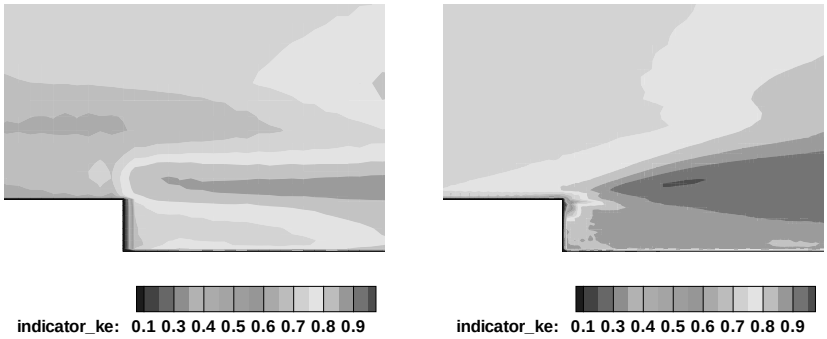

Figure 6 Flow over a backward-facing step at $Re_h = 37500$ by [4]: Sensor based on the resolved turbulent kinetic energy (1) on medium mesh (left) and on a fine mesh (right) using the Smagorinsky model and wall-functions.

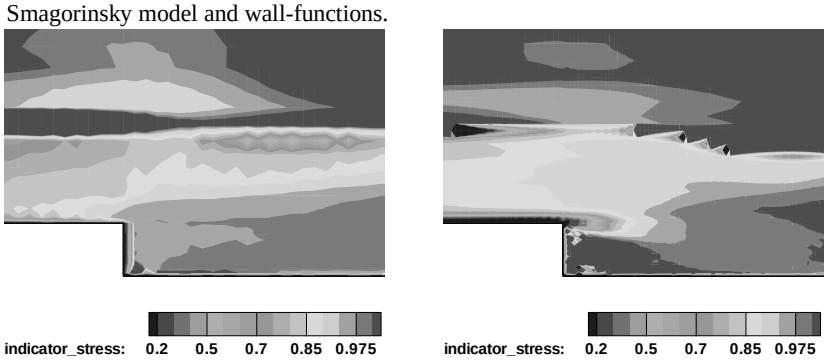

Figure 7 Flow over a backward-facing step at $Re_h = 37500$ by [4]: Sensor based on the resolved turbulent shear stress (2) on medium mesh (left) and on a fine mesh (right) using the Smagorinsky model and wall-functions.

Institut für Numerische und Angewandte Mathematik
Universität Göttingen
Lotzestr. 16-18
D - 37083 Göttingen

Telefon: 0551/394512
Telefax: 0551/393944

Email: trapp@math.uni-goettingen.de URL: http://www.num.math.uni-goettingen.de

Verzeichnis der erschienenen Preprints 2008:

2008-01	M. Körner, A. Schöbel	Weber problems with high-speed curves
2008-02	S. Müller, R. Schaback	A Newton Basis for Kernel Spaces
2008-03	H. Eckel, R. Kress	Nonlinear integral equations for the complete electrode model in inverse impedance tomography
2008-04	M. Michaelis, A. Schöbel	Integrating Line Planning, Timetabling, and Vehicle Scheduling: A customer-oriented approach
2008-05	O. Ivanyshyn, R. Kress, P. Serranho	Huygen's principle and iterative methods in inverse obstacle scattering
2008-06	F. Bauer, T. Hohage, A. Munk	Iteratively regularized Gauss-Newton method for nonlinear inverse problems with random noise
2008-07	R. Kress, N. Vintonyak	Iterative methods for planar crack reconstruction in semi-infinite domains
2008-08	M. Uecker, T. Hohage, K.T. Block, J. Frahm	Image reconstruction by regularized nonlinear inversion - Joint estimation of coil sensitivities and image content
2008-09	M. Schachtebeck, A. Schöbel	IP-based Techniques for Delay Management with Priority Decisions
2008-10	S. Cicerone, G. Di Stefano, M. Schachtebeck, A. Schöbel	Dynamic Algorithms for Recoverable Robustness Problems
2008-11	M. Braack, G. Lube	Finite elements with local projection stabilization for incompressible flow problems
2008-12	T. Knopp, X.Q. Zhang, R. Kessler, G. Lube	Calibration of a finite volume discretization and of model parameters for incompressible large eddy-type simulations
2008-13	P. Knobloch, G. Lube	Local projection stabilization for advection-diffusion-reaction problems: One-level vs. two-level approach

2008-14	G. Lube, B. Tews	Distributed and boundary control of singularly perturbed advection-diffusion-reaction problems
2008-15	G. Lube, B. Tews	Optimal control of singularly perturbed advection-diffusion-reaction problems
2008-16	M. Weyrauch, D. Scholz	Computing the Baker-Campbell-Haussdorff series and the Zassenhaus product
2008-17	A. Schöbel, D. Scholz	The big cube small cube solution method for multidimensional facility location problems
2008-18	X. Zhang, T. Knopp, M. Valentino, R. Kessler, G. Lube	Investigation of resolution requrements for wall-modelled LES of attached and massively separated flows at high Reynolds numbers

latex hinten-2008.tex